energies

MDPI

Article

Optimal Energy Consumption Path Planning for Quadrotor UAV Transmission Tower Inspection Based on Simulated Annealing Algorithm

Min Wu *, Wuhua Chen and Xiaohong Tian

School of Electrical Engineering, Guangxi University, Nanning 530004, China
* Correspondence: dr_wu2022@foxmail.com

Abstract: In order to improve the efficiency of UAVs in transmission tower inspections, the UAV transmission tower inspection energy consumption model is proposed for the existing research in which there is no accurate energy consumption calculation method in transmission tower inspection, and the optimal energy consumption path for UAV transmission tower inspection is designed by combining with simulated annealing algorithm. Firstly, a real experimental environment is built for experimental data collection and analysis, and the energy consumption model for transmission tower inspection is constructed and the influencing factors are discussed and analyzed, and the energy consumption coefficients under different situations are obtained. Second, according to the constructed transmission tower inspection energy consumption model combined with the path planning algorithm, experimental simulation is conducted to plan the optimal energy consumption inspection path, and finally, the above results are verified by carrying out actual measurement experiments. The simulation results show that under different constant loads, the optimal energy consumption path in this paper can save 36.53% and 27.32% compared with the conventional path; compared with the shortest path, it can save 11.16% and 0.45%. The optimal energy consumption path of UAV transmission tower inspection based on the simulated annealing algorithm proposed in this paper effectively improves the efficiency of UAV transmission tower inspection.

Keywords: UAV; transmission tower inspection; energy consumption model; path planning

check for updates

Citation: Wu, M.; Chen, W.; Tian, X. Optimal Energy Consumption Path Planning for Quadrotor UAV Transmission Tower Inspection Based on Simulated Annealing Algorithm. *Energies* **2022**, *15*, 8036. https://doi.org/10.3390/en15218036

Academic Editors: Xiang Li, Shenwang Li, Dongdong Zhang and Lina Yang

Received: 10 July 2022
Accepted: 5 September 2022
Published: 28 October 2022

Publisher's Note: MDPI stays neutral with regard to jurisdictional claims in published maps and institutional affiliations.

Copyright: © 2022 by the authors. Licensee MDPI, Basel, Switzerland. This article is an open access article distributed under the terms and conditions of the Creative Commons Attribution (CC BY) license (https://creativecommons.org/licenses/by/4.0/).

1. Introduction

Transmission towers are important fulcrums for power transmission and constitute an important element for the safe, reliable and stable operation of the lines. Regular inspections of transmission towers require a clear understanding of the entire tower and the elimination of potential faults to ensure the reliability of the power supply to the power system. However, the traditional manual inspection method requires maintenance personnel to climb towers and detours to detect transmission towers, which has the disadvantages of high risk factors, high operational intensity and low efficiency [1–3].

The quadrotor UAV has the advantages of low cost, small size and high mobility, and can enter dangerous areas for non-contact comprehensive inspection [4–6]. Through the ground staff's control of the UAV to the transmission tower to be inspected in order to collect, observe and identify the operational status information and compare the relevant data, any damages and defects to the transmission tower equipment [7–9] can be quickly and accurately found, in order to ensure the safe operation of the power equipment.

However, UAV inspection operations are limited by battery capacity and limited inspection radius distance. Therefore, it is important to study how to improve the efficiency of UAV battery utilization to ensure the successful completion of transmission tower inspection tasks. At present, domestic and foreign scholars have carried out certain research work on this aspect [10]. Domestic research scholars Fan Yeman et al. [11] designed the steering energy consumption test system of UAVs to analyze the total energy consumption

and average angular velocity data and conducted experimental tests to derive the relationship between the total energy consumption generated during steering and its steering angular velocity. Dong Fang et al. [12] proposed an accurate energy consumption model for UAVs and established the relationship between the relevant parameters during flight and the energy consumption generated by UAVs. Zhang Shi Xun et al. [13] discussed the influencing factors affecting the duration of the quadrotor UAV and estimated the UAV duration by mathematical modeling, propeller modeling, motor modeling, ESC modeling and battery modeling [14]. Xu Suijia [15] studied the energy consumption law based on plant protection UAVs in agricultural applications and analyzed the energy consumption law at different stages and flight speeds by collecting experimental data for polynomial fitting [16,17].

The UAV energy consumption calculation methods are mainly divided into two categories: "black box" and "white box". Regarding the "white box" method, Liu et al. [18] modeled the UAV, estimated the model parameters, and finally brought the parameters into the theoretical model for calculation to establish a theoretical power consumption model of the UAV. Bezzo et al. [19] took into account the transition process between UAV motion processes, while applying the interpolation function method to solve for energy consumption and applied their results to real-time path planning for UAV operations to find the path with the least energy consumption. Abdilla et al. [20] predicted the flight time by modeling the UAV battery characteristics, but the method is too dependent on the type of battery and is not applicable to all types of UAVs, so there are some limitations. In general, the shortcoming of the "white box" method is that it requires the estimation of the physical parameters of the UAV, such as propeller efficiency, motor efficiency, and air drag coefficient, but wind tunnel tests are required to obtain accurate parameters, which can easily lead to low accuracy of the calculated energy consumption.

Compared to the "white box" approach, the "black box" approach is a fast modeling method characterized by a theoretical model that does not require estimation of any physical parameters and only requires the application of a small number of measurable variables and physical parameters of the UAV [21]. This modeling method depends only on the input variables and the desired output results, which makes it easier to process and optimize the data and can improve the accuracy of energy consumption calculation to a certain extent. The black box modeling method was used by Maekawa et al. [22] in the horizontal flight of UAVs, using the flight speed and the load weight as input variables and the output variables as energy consumption values. proposed a "black box" approach that includes three processes: data collection, data preprocessing, and data analysis, and the results are obtained using the Sklearn's regression analysis method after the data collection is completed.

Although all the above methods are effective in estimating the energy consumption of UAVs, the factors considered in the construction of UAV energy consumption models are not comprehensive enough.

In summary, most of the studies by domestic and foreign scholars on UAV path planning problems are about industrial applications or applications for the military, mainly considering the interference of obstacles and improving safety. Moreover, in power inspection there are few studies on UAV path planning on transmission poles. Therefore, it is very necessary to carry out the optimal energy consumption path planning of UAV transmission towers based on the UAV's own condition constraints, which can improve the efficiency of UAVs during transmission tower inspection and can significantly promote the intelligent development of China's power grid business [23,24].

2. UAV Transmission Tower Inspection Energy Consumption Model Construction

In order to obtain the relationship between the energy consumption generated by the UAV when inspecting the transmission towers and the flight state, this paper builds a real experimental environment and analyzes and constructs an energy consumption model by collecting experimental data. The experiment uses a self-built UAV with a flight controller

model DJA2, a total mass of 2.027 kg and a battery capacity of 2200 mAh and 11.1 V. The instantaneous voltage and current flowing through the UAV can be measured by carrying an integrated measurement module on the UAV.

2.1. Energy Consumption Modeling

In the actual transmission tower inspection, the hovering time of the UAV is much less than the time of the UAV cruise, so the hovering power consumption of the UAV can be ignored, and the total power consumption of the UAV can be estimated by using the power consumption generated by the motor when the UAV does vertical and horizontal movements. In the case of constant flight conditions, the UAV can be set to perform uniform motion, consume total power as P, and fly at a uniform speed as V. According to the previous analysis of the forces on the UAV, it is assumed that $K = P/V$ and K is the proportionality factor. The following section will explore the value of K under different flight modes by collecting and analyzing the actual flight data of the UAV and conducting experiments.

Firstly, the UAV was debugged, and the following experiments were conducted after the debugging was completed. The UAV was allowed to fly horizontally at a speed of 2 m/s without load, and the UAV power data at 100 of these consecutive time points were taken, as shown in Figure 1.

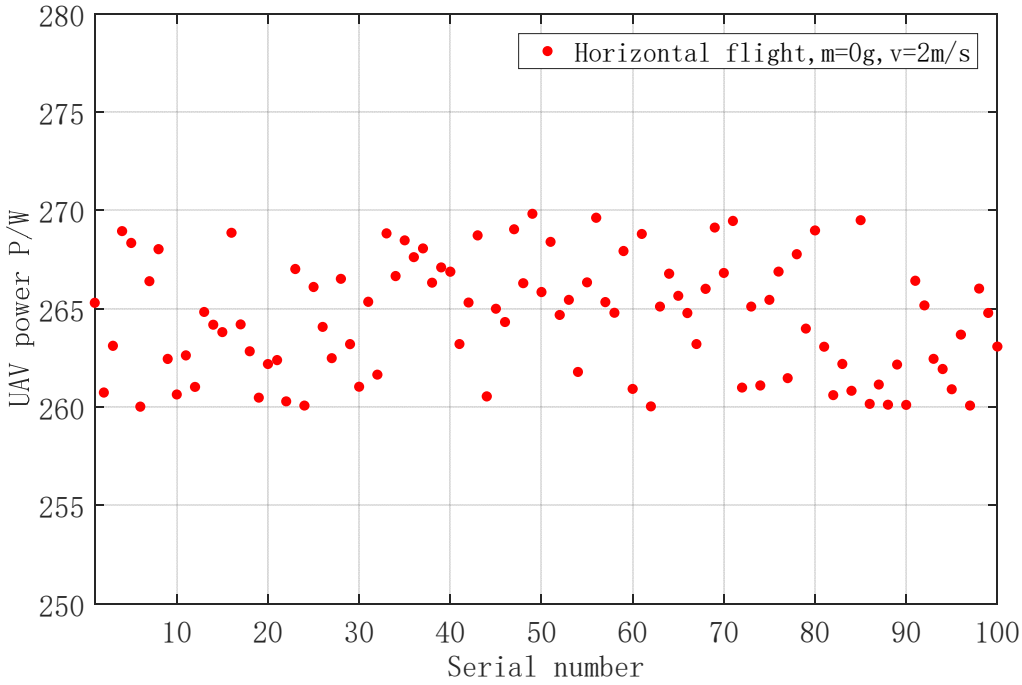


Figure 1. UAV power when no load.

From Figure 1, it can be seen that when the flight speed of the UAV is kept constant, the power fluctuation range of the UAV is small and remains almost constant. The ratio of the power of the UAV to the flight speed is the energy consumption coefficient, which is K. Therefore, it is conjectured that the energy consumption coefficient K of the UAV remains constant under the condition that the weight of the load and the flight mode remain unchanged.

The horizontal resistance coefficient is weakly related to the wind when the UAV is under low-speed condition for the tower inspection, which is usually limited from 1 m/s to 2 m/s, so we select 1 m/s and 2 m/s to verify the energy consumption coefficient K of the UAV, which remains constant under the condition that the weight of the load and the flight mode remain unchanged. In order to verify the above conjecture, let the UAV fly horizontally at 1 m/s and 2 m/s individually without load to repeat the above experiment,

take the data of 100 consecutive time points for analysis, and compare the experimental results as shown in Figure 2.

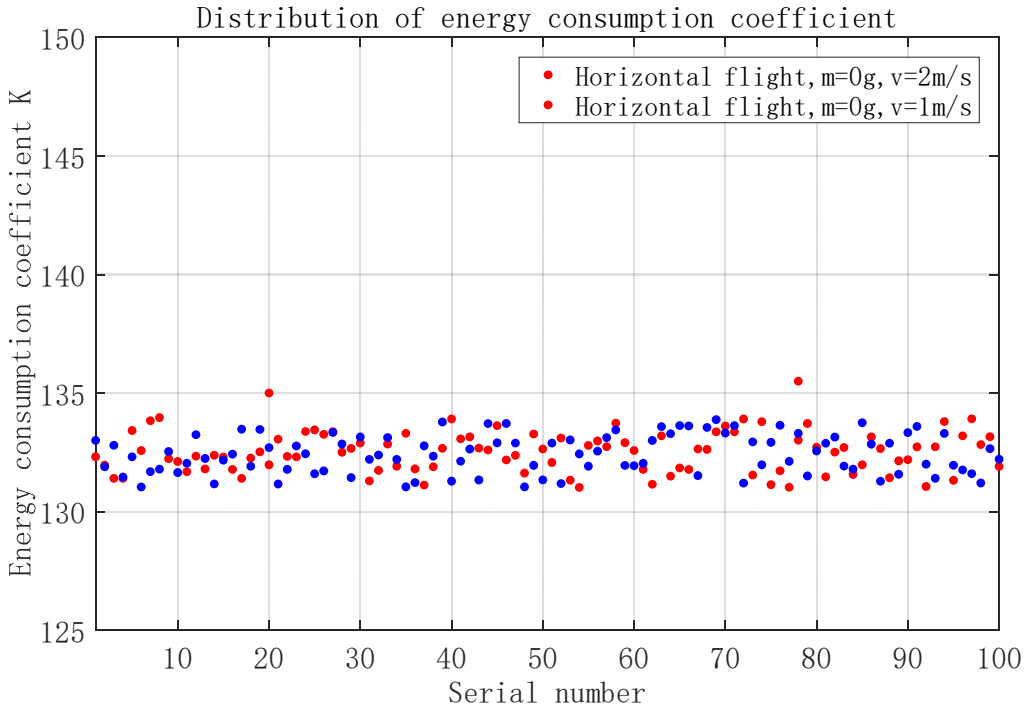


Figure 2. Distribution of energy consumption coefficient at different flight speeds.

2.2. *Analysis of Energy Consumption Impact Factors*

When the experiments in Section 2.1 were conducted, the effect on the energy consumption coefficient was discussed with the UAV flight mode and the load weight carried constant. Next, the effect of the flight mode and the load weight of the UAV on the energy consumption coefficient K will be explored [25,26].

2.2.1. Flight Mode Impact Analysis

In the flight process of UAVs, there are three states: vertical ascent, horizontal flight and vertical descent. Therefore, in this paper, experimental data are collected under these three flight modes to analyze the influence of different flight states on the energy consumption coefficient of UAVs. Firstly, the UAV was flown at a speed of 2 m/s without load in three ways: horizontal flight, vertical ascent and vertical descent, and the data were collected in 100 consecutive time points for analysis.

As can be seen from Figure 3, under the condition of keeping the same UAV load weight and flight speed, the energy consumption coefficient in the vertical ascent state is the largest, which is maintained between 140–145; the energy consumption coefficient in the horizontal flight state is the second largest, which is maintained between 130–135; and the energy consumption coefficient in the vertical descent state is the smallest, which is maintained between 118–123. Accordingly, it can be concluded that the number of ascent flights of the UAV should be reduced as much as possible in the subsequent UAV transmission tower inspection path planning.

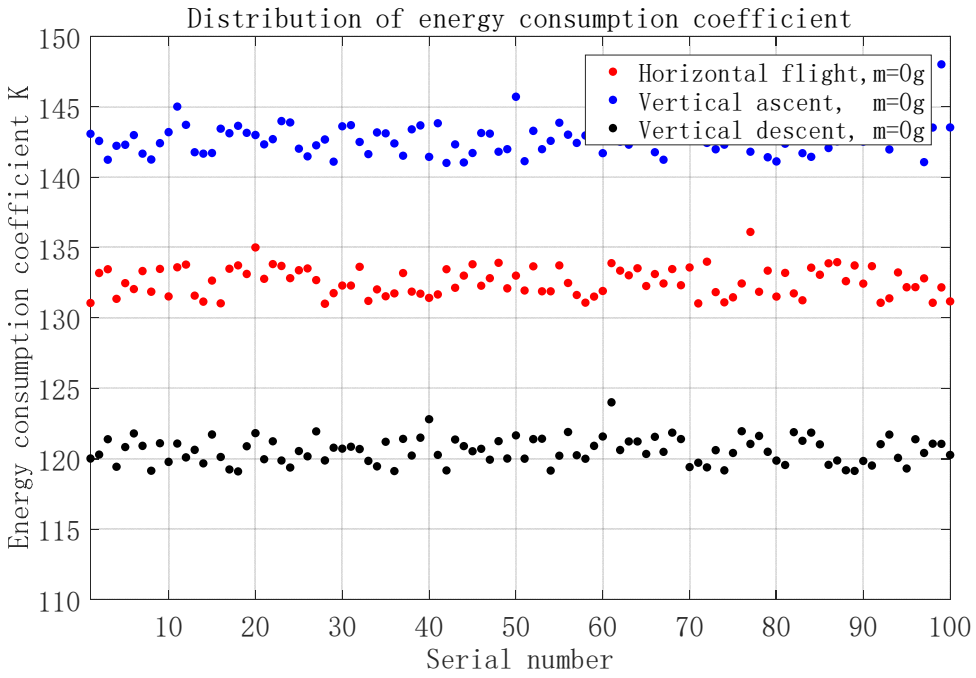


Figure 3. Distribution of energy consumption coefficient under different flight modes.

2.2.2. Load Weight Impact Analysis

In order to discuss the influence of the negative load weight on the energy consumption coefficient during the flight of the UAV, in this paper, we let the UAV keep the flight mode unchanged and fly horizontally at a speed of 2 m/s under the load of 0 g, 50 g and 100 g, respectively, and take the data of 100 of these consecutive time points for analysis and make the distribution of the energy consumption coefficient, as shown in Figure 4.

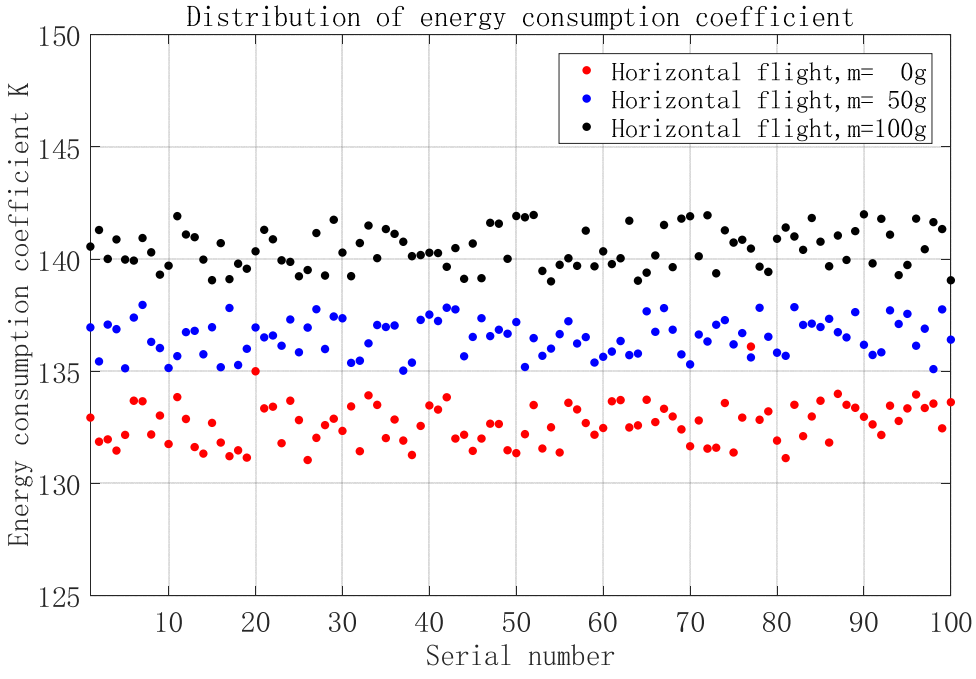


Figure 4. Distribution of flight energy consumption coefficient at different load levels.

As can be seen from Figure 4, the energy consumption coefficient increases with the increase in the UAV load weight in the horizontal flight condition and will be distributed around a stable value.

2.3. Acquisition of Energy Consumption Coefficients in Different Cases

In order to apply the UAV transmission tower inspection energy consumption model in the subsequent path planning, it is necessary to obtain the specific values of energy consumption coefficients in different cases, and to conduct horizontal flight, vertical ascent, vertical descent flight experiments at a speed of 2 m/s under 0 g, 50 g, 100 g, 150 g, 200 g, 250 g, 300 g, 350 g, 400 g, 450 g, 500 g load weights, respectively. Each type of experiment was conducted 100 times, each flight was 5 min and the data of 1000 consecutive time points were taken each time. The data in each case were simply filtered, the average value was finally taken as the energy consumption coefficient of each case, and the final energy consumption coefficient was obtained as shown in Table 1 below.

Table 1. Energy consumption coefficients under different load conditions.

Load Weight (g)	Horizontal Flight Energy Factor	Vertical Rise Energy Factor	Vertical Drop Energy Factor
0	132.320	142.419	120.986
50	136.414	146.851	124.703
100	140.566	151.347	128.473
150	144.776	155.905	132.293
200	149.062	160.545	136.183
250	153.388	165.230	140.108
300	157.771	169.979	144.084
350	162.213	174.800	148.123
400	166.713	179.667	152.193
450	171.271	184.606	156.325
500	175.886	189.609	160.509

It can be seen from Table 1 above that the energy consumption coefficients of all three flight modes will increase with the increase in the load weight, and it can also be seen that, under the same load weight, the energy consumption coefficient of the UAV in vertical ascent is the largest, in horizontal flight the second largest, and in vertical descent the smallest. At the same time, for the convenience of calculating the energy consumption of the subsequent UAV transmission tower inspection path planning, the energy consumption coefficient in the horizontal flight state is recorded as K_f, the energy consumption coefficient in the vertical ascent state is recorded as K_r, and the energy consumption coefficient in the vertical descent state is recorded as K_d in this paper.

3. UAV Transmission Tower Inspection Optimal Energy Consumption Path Planning

The inspection process can be divided into fine inspection of towers and inspection between different towers when the UAV is inspecting transmission towers. For this reason, this paper will design flight paths for different inspection tasks, which are divided into path planning between transmission towers and flight around towers.

3.1. UAV Inspection of Regional Type Transmission Tower Model Construction

In order to obtain the actual scene of UAV inspection in transmission towers, the geographic location information of each tower in the inspection area, including the latitude and longitude coordinates and elevation of each tower, can be known by consulting the relevant data. In order to make the path planning of the UAV convenient when inspecting the transmission towers, a three-dimensional map of the inspection area is first constructed by using the Digital Elevation Model (DEM), and then the latitude and longitude of the geographical location are converted by using the local central meridian as the reference for coordinates. Tower 1 is set as the inspection starting point, and the 3D model of a total of 40 target inspection points is obtained for path planning. The constructed three-dimensional mathematical model of inspection target points is shown in Figure 5 below.

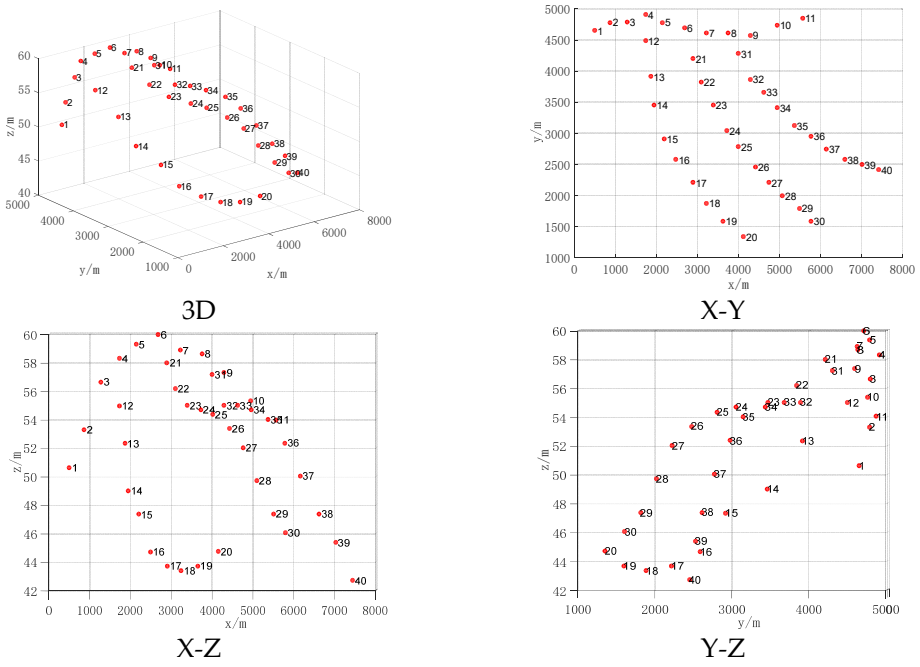


Figure 5. Regional type transmission tower inspection point three dimensional map.

3.2. Design of Path Planning Based on Simulated Annealing Algorithm

In order to facilitate the planning of the optimal path for UAV transmission tower inspection using intelligent algorithms, the operational path is first mathematically modeled and the path planning problem is transformed into a mathematical problem that can be solved by intelligent algorithms [27–29]. In this paper, the location of the target point to be inspected by the UAV is known, and the UAV inspects from the starting tower and subsequently flies to the remaining towers. In this process, the UAV only needs to reach the target inspection tower once and fly to the starting tower after completing the inspection task. In order to minimize the total energy consumption generated by the UAV during the whole inspection process, the flight path of the UAV needs to be planned. This is then converted into a mathematical application problem, which is to search for an arrangement of the natural subset $X = \{1, 2, \ldots, n\}$ (the elements of X which correspond to the number of each pole tower point corresponding to the entire cruise mission) such that the value taken in Equation (1) is minimized.

$$T_d = \sum_{i=1}^{n-1} d(V_i, V_{i+1}) + d(V_n, V_1) \tag{1}$$

where T_d is the total energy consumption generated after inspection of all transmission towers, $d(V_i, V_{i+1})$ is the energy consumption generated during the whole flight from transmission tower V_i to transmission tower V_{i+1}, KJ.

In order to calculate the process energy consumption $d(V_i, V_{i+1})$ of the UAV flying from the current target tower to the next target tower, based on the relative flight distance and the energy consumption coefficient, the calculation formula is:

$$d(V_i, V_{i+1}) = \begin{cases} |d_x|K_f + |d_y|K_f + |d_z|K_r (d_z \geq 0) \\ |d_x|K_f + |d_y|K_f + |d_z|K_d (d_z \leq 0) \end{cases} \tag{2}$$

Among them.

$$\begin{cases} d_x = X_{i+1} - X_i \\ d_y = Y_{i+1} - Y_i \\ d_z = Z_{i+1} - Z_i \end{cases} \tag{3}$$

where d_x, d_y, d_z are the distances between the current target tower and the next target tower in the x, y, and z directions, m; (X_i, Y_i, Z_i) are the coordinates of the current target tower; $(X_{i+1}, Y_{i+1}, Z_{i+1})$ are the coordinates of the next target tower.

To solve the optimal path for energy consumption, the optimization search is based on the simulated annealing algorithm (SAA). This algorithm can find the global optimal solution with high probability and has strong robustness, global convergence, implied parallelism and wide adaptability. The key core of this algorithm is the Metropolis discriminant criterion, which in this study is specified as:

$$D = \begin{cases} 1(df < 0) \\ \exp\left(-\frac{df}{T}\right)(df \geq 0) \end{cases} \tag{4}$$

Among them.

$$df = T_{new} - T_{old} \tag{5}$$

where D is the probability that the Metropolis discriminant criterion finally accepts the new path; T_{new} is the total flight energy consumption of the new path, KJ; T_{old} is the total flight energy consumption of the previous path, KJ; T is the algorithm control parameter, i.e., the current temperature.

From Equation (4), if $df < 0$, the new path is accepted with probability 1; otherwise, the new path is accepted with probability exp $(-df/T)$.

When solving the optimal energy consumption path based on the simulated annealing algorithm, the algorithm is first initialized, i.e., the coordinate information of the target point is input and the control parameters of the algorithm itself are assigned, at which time the coordinate information contains the energy cost of the process of flight between the two target points of the UAV under different load conditions. After the initialization of the algorithm is completed, the path search is started, and the new path is accepted using the discriminant criterion of Equation (4), and the acquisition of the optimal energy consumption path is finally completed. In the optimization process, let $T = qT$, i.e., each cycle shrinks the current temperature T by q times as the next current temperature. The algorithm flow is shown in Figure 6 below.

In order to improve the solution performance of the simulated annealing algorithm in this study, by referring to the control parameters commonly used in this algorithm and conducting several experiments on the problem in this study, the control parameters were finally selected as follows: initial temperature T_0 = 1000; termination temperature T_{end} = 0.001; chain length L = 500; cooling rate q = 0.9.

3.3. UAV Refinement Inspection of Transmission Towers

3.3.1. Refine Transmission Tower Inspection Content

Refined inspection usually refers to the operation of multi-rotor UAVs to a fixed-point hovering way of image photography of the tower itself and the key parts of the ancillary facilities, in order to check the line defects, hidden dangers and other abnormal state. Combined with the national grid company line inspection management norms, this paper takes the most common AC single-return linear tower as an example to elaborate on the content of fine inspection, inspection content as shown in Table 2.

Table 2. AC single-return linear tower refinement inspection content.

Number	Project Name	Number of Photos Taken
1	Pole Tower Signage	1
2	Left phase insulators	3
3	Medium phase insulators	3
4	Right phase insulator	3
5	Left ground suspension point	1
6	Right ground suspension point	1

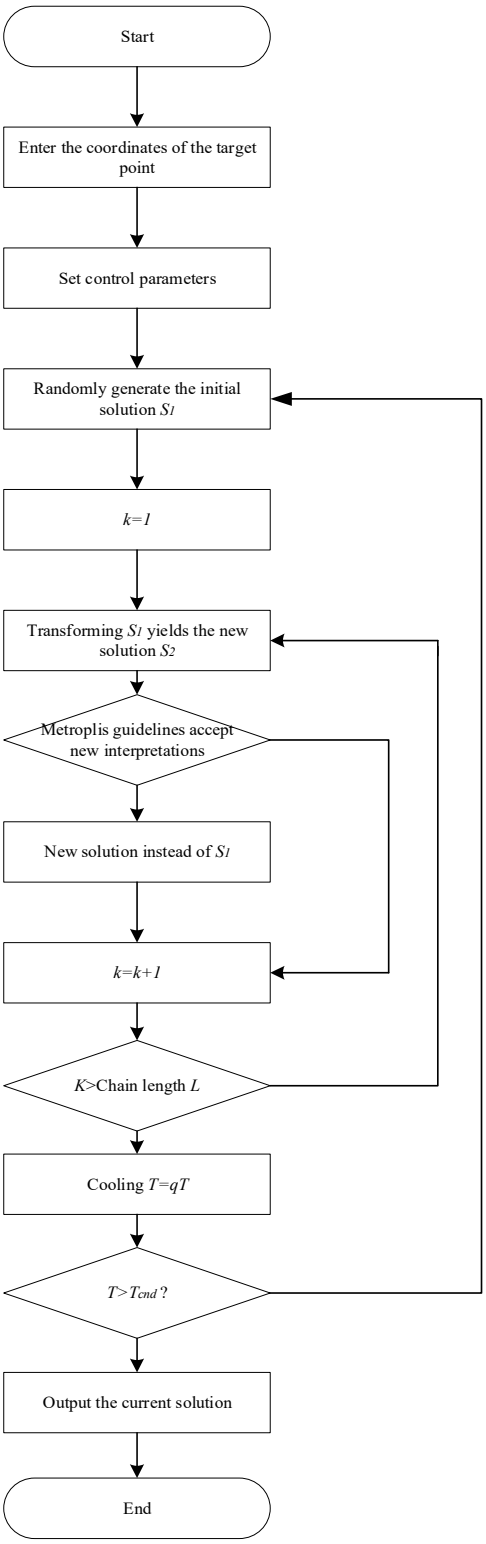


Figure 6. Flow chart of transmission tower path planning algorithm solution.

As can be seen from Table 2, for each AC single-return linear tower, there are 6 inspection items and a total of 12 photos are taken, including the main tower components such as tower signage, left phase insulator, right phase insulator, middle phase insulator, left ground wire suspension point and right ground wire suspension point.

3.3.2. Fine-Tuning Tower Inspection Strategy

This paper takes a 500 kV AC single-return linear transmission tower as the research object, as shown in Figure 7, and the part marked by a red circle needs to be photographed during the UAV inspection. Each insulator string contains 14 pieces of insulators, and the length of each insulator is 146 mm, while the length of the whole insulator string is $14 \times 146 = 2044$ mm. The error size caused by the connection joint of the insulator string and the tilt of the insulator string is negligible.

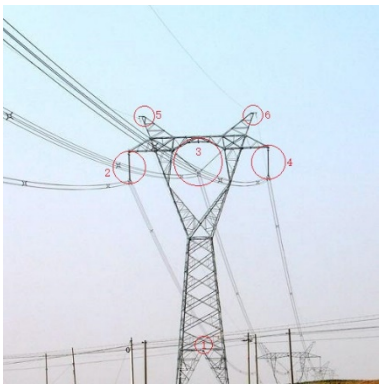


Figure 7. AC single-return linear transmission tower diagram.

In order to avoid the impact of strong electromagnetic fields near high-voltage power lines on the UAV's on-board electronic equipment during the inspection process, the minimum distance between the UAV for transmission tower inspection and the tower is defined as the safety distance S. Outside the safety distance, the UAV can effectively avoided electromagnetic field interference to ensure the safe completion of the inspection task. UAVs can carry a variety of different sensors or cameras for detection when conducting transmission tower inspections. The field of view (FOV) angle of the on-board monitoring camera is expressed as α. The vertical distance from the UAV to the target transmission tower is expressed as L. Its effective monitoring range is shown in Equation (6).

$$R = L \times \tan\left(\frac{\alpha}{2}\right) \tag{6}$$

The HD10X remote zoom camera was selected for this article. The camera itself weighs 130 g, the horizontal field of view range is 53.2° (near focal length) to 5.65° (far focal length), and the vertical field of view angle range is 39.8° (near focal length) to 4.2° (far focal length). After several tests, it is concluded that the camera not only has a clear picture in the 6× zoom range, but also has good anti-shock performance, which meets the inspection requirements of the UAV for transmission towers. According to the regulations of transmission line inspection, the safety distance of the 500 kV transmission line is set to S = 8 m. For better safety consideration, this paper selects L = 10 m (L > S) and uses a 6× zoom camera for photo processing; in this case, the actual detection range of the camera is

$$R_1 = L\tan\left(\frac{\alpha}{2}\right) = 10 \times \tan\left(\frac{21.28}{180}\pi/2\right) = 1.8787m \tag{7}$$

$$R_2 = L\tan\left(\frac{\alpha}{2}\right) = 10 \times \tan\left(\frac{15.92}{180}\pi/2\right) = 1.3983m \tag{8}$$

Because the length of insulator string is 2044 mm, each insulator string needs to take at least two photos to detect the whole insulator. In this paper, we choose to take three photos at each insulator string in order to get a more detailed photo.

3.3.3. Refine the Tower Inspection Process

In the inspection of a single transmission tower, this paper takes into account the influence of various factors such as the safety distance, the camera shooting distance and the wiring near the transmission tower during the UAV inspection, and summarizes the following safe and reliable inspection process, as shown in Figure 8.

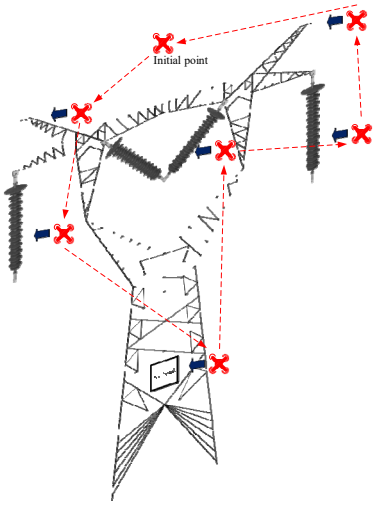


Figure 8. Diagram of the fine inspection process of the tower.

As can be seen in Figure 8, the UAV inspection is initially located directly above the tower and inspects it sequentially in accordance with the direction marked by the red dotted line.

4. Analysis and Justification of Experimental Results

4.1. Regular Route Planning Results

As can be seen from Figure 9 above, the motion process of the UAV under the "Z" inspection path is analyzed and the total energy consumption of the flight under different load weights is calculated. The numerical results of the total energy consumption generated by the UAV in the conventional operation path under different load weights are shown in Table 3 below.

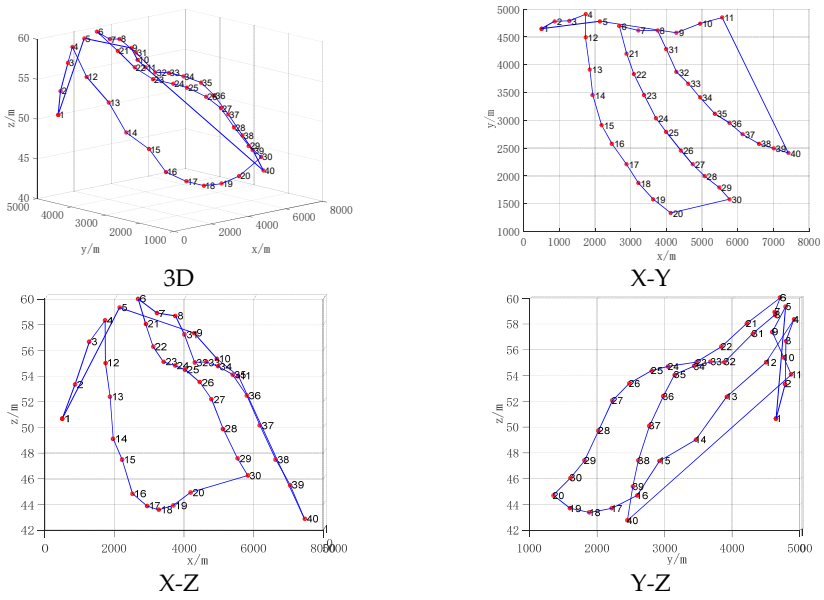


Figure 9. UAV conventional operation path diagram.

Table 3. Total energy consumption of UAV flight under different paths.

Load Weight (g)	Regular Path (J)	Shortest Path (J)	Energy Consumption Optimal Path (J)
0	1.1721 × 109	0.8713 × 109	0.7602 × 109
50	1.2083 × 109	0.8822 × 109	0.8362 × 109
100	1.2451 × 109	0.9091 × 109	0.8444 × 109
150	1.2824 × 109	0.9363 × 109	0.8525 × 109
200	1.3204 × 109	0.9640 × 109	0.8744 × 109
250	1.3587 × 109	0.9920 × 109	0.8935 × 109
300	1.3975 × 109	1.0203 × 109	0.9072 × 109
350	1.4368 × 109	1.0490 × 109	0.9373 × 109
400	1.4767 × 109	1.0781 × 109	0.9743 × 109
450	1.5171 × 109	1.1076 × 109	1.0345 × 109
500	1.5580 × 109	1.1375 × 109	1.1324 × 109

4.2. Shortest Path Planning Results

As can be seen from Figure 10 above, by analyzing the motion process of the UAV under the shortest distance inspection path and calculating its total flight energy consumption generated under different load weights, the numerical results of the total energy consumption generated by the UAV in the shortest distance operation path under different load weights are obtained, as shown in Table 3 below.

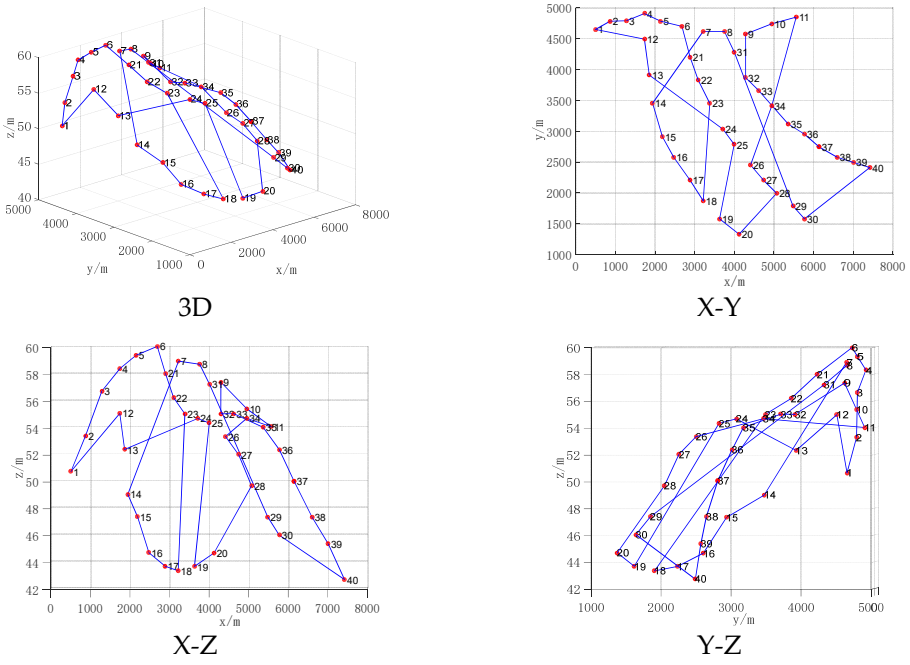
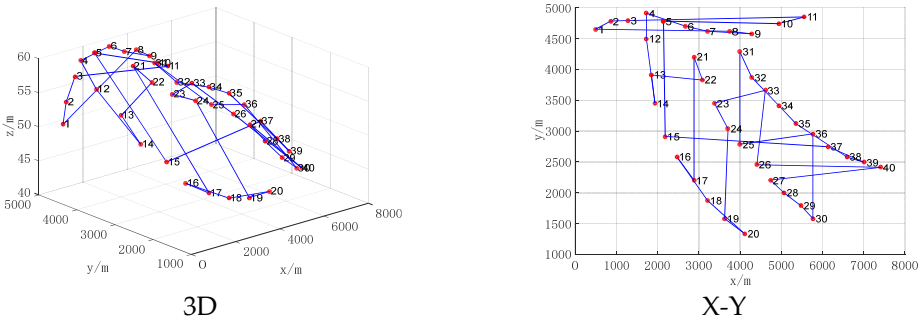
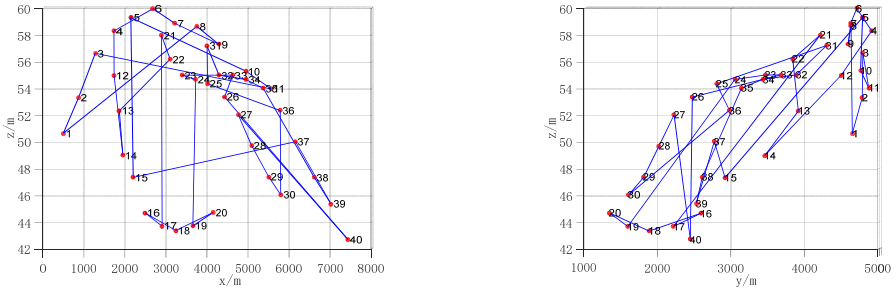


Figure 10. UAV shortest distance operation path.

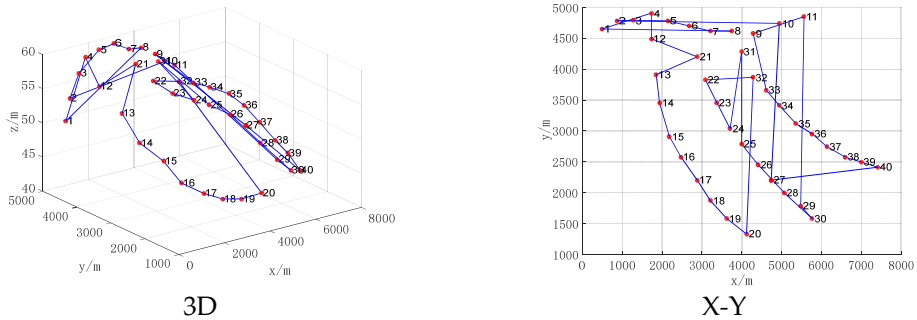
4.3. Energy Consumption Optimal Path Planning Results

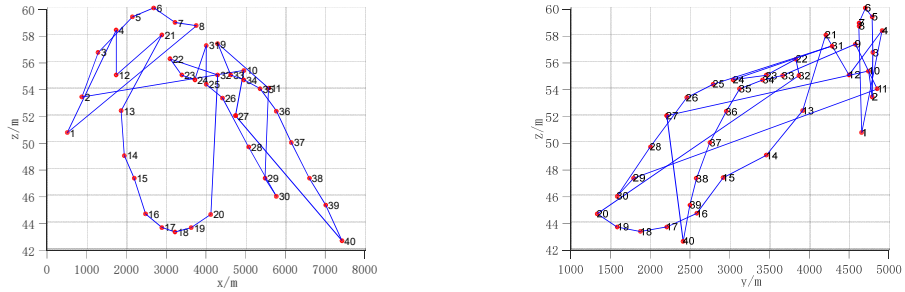
The energy-optimal path finding for the operational target is based on the simulated annealing algorithm, in which the flight distance of the UAV is not considered and only the algorithm is used to obtain the energy-optimal path of the UAV traversing all target points in flight. The path planning experiment is carried out and the results of the algorithm for different constant load cases of the UAV are shown in Figure 11 below.





(**a**)





(**b**)

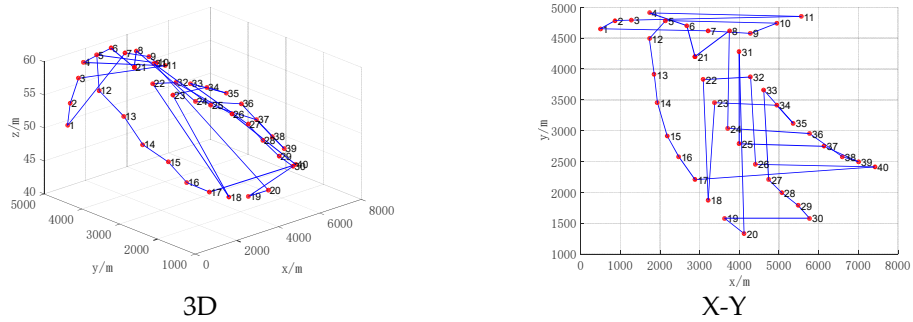
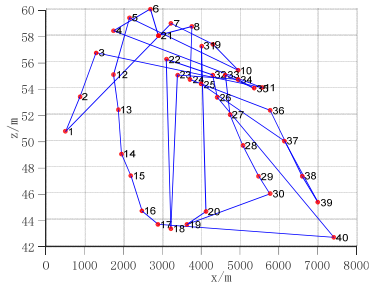
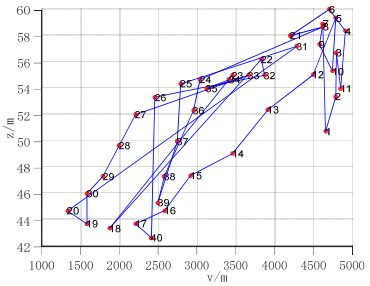


Figure 11. *Cont.*

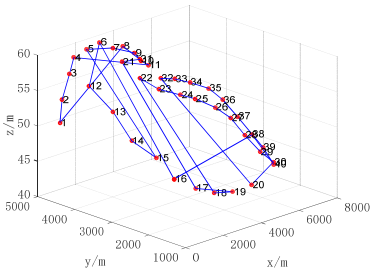


X-Z

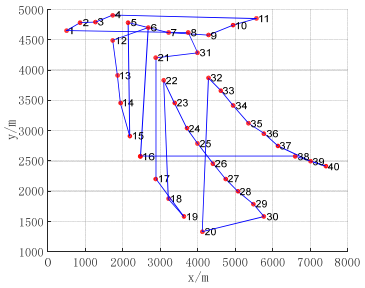


Y-Z

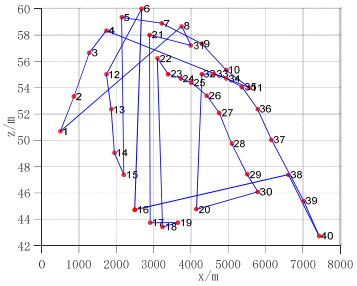
(**c**)



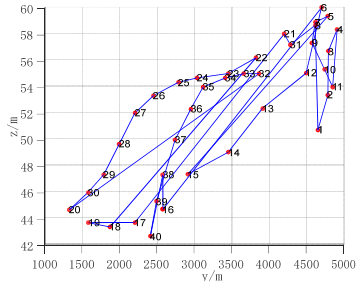
3D



X-Y

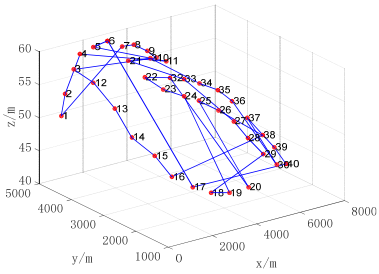


X-Z

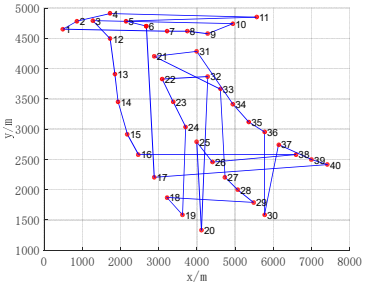


Y-Z

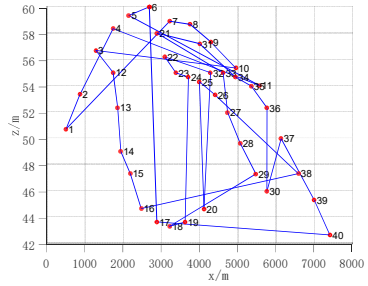
(**d**)



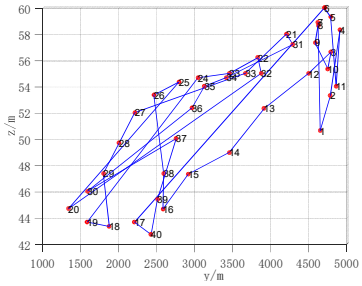
3D



X-Y



X-Z



Y-Z

(**e**)

Figure 11. *Cont*.

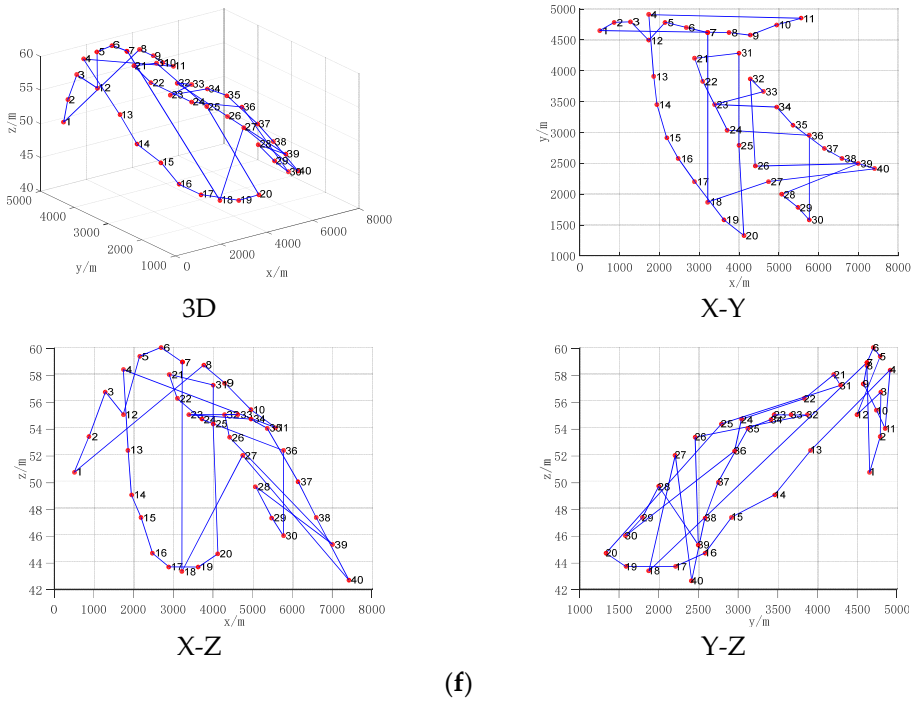


Figure 11. (**a**) Optimal energy consumption operation path at load 0 g; (**b**) Optimal energy consumption operation path at 100 g load; (**c**) Optimal energy consumption operation path at 200 g load; (**d**) Optimal energy consumption operation path at 300 g load; (**e**) Optimal energy consumption operation path at 400 g load; (**f**) Optimal energy consumption operation path at 500 g load.

As can be seen from Figure 11, the paths planned by the algorithm for the UAV under various different constant loads are similar in that they all ensure that the UAV flies from the starting point to the lower altitude target point as a priority, i.e., it generates a descent motion as a priority, then operates at an intermediate altitude as much as possible, and finally completes the target point operation at the higher position, thus returning to the starting position.

4.4. Analysis of Path Planning Results

By analyzing the flight process of the UAV under the "Z" path, the shortest path and the optimal energy consumption path, the total energy consumption of the flight under different load conditions is calculated, and the results are shown in Table 3.

By analyzing the results of the total energy consumption of the above UAVs flying on different paths under different conditions, the total energy consumption of the conventional path and the shortest operating path are used as references to calculate the energy consumption savings of the optimal path planned by the simulated annealing algorithm under different load conditions, respectively, and the results are shown in Table 4.

As can be seen from Table 4, the reduction in total flight energy consumption for the energy-optimal path compared to the conventional path is large, with a minimum of 26.76% and a maximum of 32.04%. For the shortest path, the reduction of total flight energy consumption in the case of constant load is small, with a maximum of 5.47%. The load of the UAV during a single flight is constant, but different flights can have different loads. The reduction of total flight energy consumption is larger, at 11.72%. Table 4 illustrates that the method we proposed has less energy consumption compared with the conventional and the shortest path, but the energy savings fluctuate randomly because of the influence of both aerodynamic force and fly control.

Table 4. Comparison of energy consumption of optimal path and other paths.

Load Weight (g)	Energy Savings with Conventional Paths/%	Energy Savings Over Shortest Path/%
0	35.14%	11.16%
50	30.80%	5.21%
100	32.18%	7.12%
150	33.52%	8.95%
200	33.78%	9.30%
250	34.24%	9.93%
300	35.08%	11.08%
350	36.86%	10.65%
400	36.53%	9.63%
450	31.81%	6.60%
500	27.32%	0.45%

5. Conclusions

This paper constructs an UAV transmission tower inspection energy consumption model construction and optimizes its model parameters. An experimental test plan for the UAV energy consumption model is given, an experimental environment and test platform are built, hypotheses are proposed for the UAV energy consumption model, and then the model is verified and analyzed through experiments to verify the accuracy of the model. At the same time, the optimal energy consumption path planning method for transmission tower inspection based on energy consumption constraints is proposed. Combined with the geographic location information of the pole tower, its three-dimensional mathematical model is constructed, the path planning problem is converted into a TSP problem, and the optimal energy consumption path planning is realized by simulated annealing algorithm. In summary, the UAV can basically use the shortest path to replace the energy-optimal path for operation when operating with constant load, but for the UAV operation with real-time changes in load, the energy-optimal path should be used for operation to reduce the total energy consumption of the UAV flight during operation, so as to improve the operation efficiency.

Author Contributions: Investigation, Writing—original draft, M.W., W.C. and X.T. All authors have read and agreed to the published version of the manuscript.

Funding: This research received no external funding.

Institutional Review Board Statement: Not applicable.

Informed Consent Statement: Not applicable.

Data Availability Statement: Not applicable.

Conflicts of Interest: The authors declare no conflict of interest.

References

1. Peng, X.; Qian, J.; Mai, X. Automatic Power Line Inspection Technology of Large Unmanned Helicopter and Its Application. *South. Power Syst.Technol.* **2016**, *10*, 24–31.
2. Peng, X.; Chen, C.; Xiaogang, X.; Wenxue, X.; Wang, K.; Yang, B.; Mai, X. Safe distance diagnosis technology for power transmission channel based on UAV laser scanning. *Power Syst. Technol.* **2014**, *38*, 1–15.
3. Liu, Z.; Du, Y.; Chen, Y.; Ma, J.G. Simulation and Experiment on the Safety Distance of Typical ±500 kV DC Transmission Lines and Towers for UAV Inspection. *Gaodianya Jishu/High Volt. Eng.* **2019**, *45*, 426–432.
4. Baena, S.; Boyd, D.S.; Moat, J. UAVs in pursuit of plant conservation—Real world experiences. *Ecol. Inform.* **2018**, *47*, 2–9. [CrossRef]
5. Yu, T.; Wang, X.; Jin, J.; McIsaac, K. Cloud-Orchestrated Physical Topology Disco-very of Large-Scale IoT Systems Using UAVs. *IEEE Trans. Ind. Inform.* **2018**, *14*, 2261–2270. [CrossRef]
6. Simic, M.; Bil, C.; Vojisavljevic, V. Investiga-tion in Wireless Power Transmis-sion for UAV Charging. *Procedia Comput. Sci.* **2015**, *60*, 1846–1855. [CrossRef]

7. Sampedro, C.; Rodriguez-Vazquez, J.; Rodriguez-Ramos, A.; Carrio, A.; Campoy, P. Deep Lear-ning-Based System for Automatic Recognition and Diagnosis of Electrical Insulator Strings. *IEEE Access* **2019**, *7*, 101283–101308. [CrossRef]
8. Shao, G.; Liu, Z.; Fu, J.; Tan, J.Y.; Chen, Y.; Zhou, L.W. Research Progress in Unmanned Aerial Vehicle Inspection Technology on Overhead Transmission Lines. *High Volt. Eng.* **2020**, *46*, 14–22.
9. Li, J.; Duan, Y.; Wang, C. The application of drones in transmission line inspection. *Power Syst. Clean Energy* **2017**, *33*, 62–65, 70.
10. Prasetia, A.S.; Wai, R.J.; Wen, Y.L.; Wang, Y.K. Mission-Based Energy Consumption Prediction of Multirotor UAV. *IEEE Access* **2019**, *7*, 33055–33063. [CrossRef]
11. Fan, Y.; Wang, D.; Shen, K.; Zhang, H.H. Design and test of steering energy consumption test system for electric multi-rotor UAV. *Sci. Technol. Eng.* **2019**, *19*, 126–131.
12. Dong, F.; Wu, M.; Zhu, W. Energy-optimized UAV flight planning for IoT environments. *J. Southeast Univ. Nat. Sci. Ed.* **2020**, *50*, 150–157.
13. Zhang, Z.; Xia, Q.; Cao, Y. Range optimization for multi-rotor UAVs. *Ordnance Ind. Autom.* **2020**, *39*, 93–96.
14. Zhang, D.; Zhu, H.; Zhang, H.; Goh, H.H.; Liu, H.; Wu, T. Multi-objective optimization for smart integrated energy system considering demand responses and dynamic prices. *IEEE Trans. Smart Grid* **2022**, *13*, 1100–1112. [CrossRef]
15. Zhang, X.; Xu, S.; Wang, Y.; Liu, S.; Qiao, Y. Experimental study on the energy consumption law of plant protection drones. *Int. Agric. Eng. J.* **2019**, *28*, 1–7.
16. Ahmad, T.; Zhang, D.; Shah, W.A. Efficient energy planning with decomposition-based evolutionary neural networks. *IEEE Access* **2020**, *8*, 134880–134897. [CrossRef]
17. Zhang, D.; Liu, T. A multi-step modeling and optimal operation calculation method for large-scale energy hub model considering two types demand responses. *IEEE Trans. Smart Grid* **2019**, *10*, 6735–6746. [CrossRef]
18. Liu, Z.; Sengupta, R.; Kurzhanskiy, A. A power consumption model for multi-rotor small unmanned aircraft systems. In Proceedings of the 2017 International Conference on Unmanned Aircraft Systems (ICUAS), Miami, FL, USA, 13–16 June 2017.
19. Bezzo, N.; Mohta, K.; Nowzari, C.; Lee, I.; Kumar, V.; Pappas, G. Online planning for energy-efficient and disturbance-aware UAV operations. In Proceedings of the 2016 IEEE/RSJ International Conference on Intelligent Robots and Systems (IROS), Daejeon, Korea, 9–14 October 2016.
20. Abdilla, A.; Richards, A.; Burrow, S. Power and endurance modelling of battery-powered rotorcraft. In Proceedings of the 2015 IEEE/RSJ International Conference on Intelligent Robots and Systems (IROS), Hamburg, Germany, 28 September–2 October 2015.
21. Zhu, H.; Goh, H.H.; Zhang, D.; Ahmad, T.; Liu, H.; Wang, S.; Li, S.; Liu, T.; Dai, H.; Wu, T. Key technologies for smart energy systems: Recent developments, challenges, and research opportunities in the context of carbon neutrality. *J. Clean. Prod.* **2022**, *331*, 129809. [CrossRef]
22. Maekawa, K.; Negoro, S.; Taniguchi, I.; Tomiyama, H. Power Measurement and Modeling of Quadcopters on Horizontal Flight. In Proceedings of the International Symposium on Computing & Networking (CANDAR), Aomori, Japan, 19–22 November 2017; pp. 326–329.
23. Ahmad, T.; Zhu, H.; Zhang, D.; Tariq, R.; Bassam, A.; Ullah, F.; AlGhamdi, A.S.; Alshamrani, S.S. Energetics systems and artificial intelligence: Applications of industry 4.0. *Energy Rep.* **2022**, *8*, 334–361. [CrossRef]
24. Ahmad, T.; Zhang, D. A critical review on comparative global historical energy consumption and future requirement: The story told so far. *Energy Rep.* **2020**, *6*, 1973–1991. [CrossRef]
25. Liu, T.; Zhang, D.; Wu, T. Standardised modelling and optimisation of a system of interconnected energy hubs considering multiple energies—Electricity, gas, heating, and cooling. *Energy Convers. Manag.* **2020**, *205*, 112410. [CrossRef]
26. Liu, T.; Zhang, D.; Wang, S.; Wu, T. Standardized modelling and economic optimization of multi-carrier energy systems considering energy storage and demand response. *Energy Convers. Manag.* **2019**, *182*, 126–142. [CrossRef]
27. Zhang, D.; Zhu, H.; Zhang, H.; Goh, H.H.; Liu, H.; Wu, T. An optimized design of residential integrated energy system considering the power-to-gas technology with multi-functional characteristics. *Energy* **2022**, *238*, 121774. [CrossRef]
28. Zhang, D.; Li, C.; Goh, H.H.; Ahmad, T.; Zhu, H.; Liu, H.; Wu, T. A comprehensive overview of modeling approaches and optimal control strategies for cyber-physical resilience in power systems. *Renew. Energy* **2022**, *189*, 1383–1406. [CrossRef]
29. Liu, T.; Zhang, D.; Dai, H.; Wu, T. Intelligent modeling and optimization for smart energy hub. *IEEE Trans. Ind. Electron.* **2019**, *66*, 9898–9908. [CrossRef]